

Hadronic Interactions and TeV Muons in Cosmic Ray Cascades

G. Battistoni

I.N.F.N., Sezione di Milano, via Celoria 16, I-20133 Milano, Italy

Abstract

In view of the interpretation of data collected by large deep underground experiments in terms of primary Cosmic Ray physics, this work is focused on the study of the production of TeV muons in Extensive Air Showers. The review tries to point out those features of hadronic interactions that mostly affect the production of the high energy muons. A few different Monte Carlo codes are compared, with a particular attention to those based on the Regge-Gribov framework. The possibility of performing experimental tests of the proposed models is also briefly discussed.

1 Introduction

Cosmic rays of the highest energies can be observed only through their interaction with the Earth's atmosphere: the reliability of our interpretation of the features of such secondary particles, and of their relation to the characteristics of the primary particle, is necessarily related to quality of our understanding of hadron-hadron, hadron-nucleus and nucleus-nucleus interactions. This aspect is particularly stimulating for high energy physicists, since there is not yet an exact way to calculate the properties of the bulk of hadronic interactions. Also, from the experimental point of view, the productions of secondary cosmic rays at very high energies occurs in kinematic regions, or energy ranges, that have not been explored in accelerator experiments, and that will hardly be accessed even at the hadron colliders of the next generation. Therefore, Extensive Air Showers of energy $> 10^{15}$ still represent an almost unique chance to test our theoretical achievements in very high energy nuclear physics, not to speak of the region above 10^{17} eV, which is, at least now, completely out of reach of the present accelerator technology.

In the last years, new experiments, located on the earth surface or underground, have collected valuable data concerning different Extensive Air Shower (EAS) components. The question of the interpretation of these data, the choice of the best possible simulation tool, and in general the evaluation of the systematics associated to such simulations, has become crucial. This remains a fundamental point also for the future activities at the extreme high energies[1].

A decisive contribution to this discussion has come from the work carried on in the Karlsruhe group[2], concerning the maintenance and distribution of the CORSIKA code[3], which now can be interfaced to different hadronic packages. A detailed comparison of the results from these models has been presented in [4], and new progresses have been also presented at this conference[5]. There, the emphasis was given to the data collected by surface arrays, mostly the e.m. component and the low energy (Gev) muons.

The purpose of this work is to present a further complement to the discussion started in ref.[4], focusing the review on the Monte Carlo predictions which are specific for the production of very high energy muons (in the TeV range), as those collected by the large underground experiments. This is topic is of particular relevance in the indirect analysis of EAS, since TeV muons come from the decay of mesons produced in the very early stages of the cascade, and are more directly related to the properties of high energy interaction with respect to the low energy muon component.

After the pioneristic work of Utah's experiment[6] and the results from NUSEX[7] and FREJUS[8], recent experimental papers on the subject have been published by experiments at Gran Sasso, like MACRO[9, 10], and also by Soudan2[11] and KGF[12]. The MACRO data are important for the large collection area and the statistics, apart from the interest in the analysis method proposed in [10]. The relevance of KGF results is mainly the high energy selection because of the large rock overburden. Both experiment based their analyses on Monte Carlo models based on parameterizations experimental results at colliders. A critical discussion of these models is now considered mandatory. Some of these experiments, like MACRO or LVD[13], take also data in coincidence[15] with the EAS-TOP surface array[14]. For this reason, the calculation of the TeV muon component has to be studied also in correlation with other EAS components. This will be the subject of a much more complete review[16], of which the present work is just a partial anticipation.

In the next section the features of hadronic interactions which are relevant for muon production are reviewed. Then, in Section 3, the Monte Carlo generators under study are briefly described. Some results about the simulation of primary interactions are given in Section 4, while the comparison of full shower calculations are presented in Section 5. A general discussion is attempted in the Conclusions.

2 High energy muons as a probe of hadronic interactions

The high energy muons in EAS come from the decay of pions and kaons produced in the early stages of shower development. The interest is therefore in the cross sections, multiplicities and their fluctuations, for meson production in all kinds of possible hadron and nucleus interactions in the relevant energy range. A key aspect is the competition of decay and interaction of these mesons along their path in a medium with varying density profile, such as the atmosphere. Therefore, while the inelastic cross section of primaries determines the height of first interaction, the inelastic cross sections of mesons

determine the interaction length. The decay length is a function of meson energy, whose distribution is governed by the X_F distribution as resulting from meson, nucleon or nucleus collisions with air nuclei. In particular, the high X_F values (“fragmentation region”), poorly studied in accelerator experiments, are the dominant ones. Diffractive and non diffractive interactions are both to be considered.

The P_\perp distribution affects the transverse structure of muons in the showers, since the kink in the meson decay can be considered negligible. At TeV energies, geomagnetic deflection is a minor correction. A realistic calculation must take into account the correlations existing between P_\perp , energy and rapidity (or X_F). As already discussed in [17], while a simultaneous change in the interaction lengths of mesons and nucleons produces only second order effects in the eventual muon yield, variations in P_\perp are directly reflected in the calculation of the lateral distribution.

Of course, the lateral distribution is always the result of a convolution between longitudinal and transverse properties of the interaction. Calling r the displacement of a muon with respect to the shower axis, as measured at a slant distance H_{prod} from the relevant interaction, then:

$$r \sim \frac{P_\perp}{E_{\pi,K}} H_{prod} \quad (1)$$

In this simplified description the transverse momentum in the parent decay is neglected. The previous expression can be re-expressed in a more instructive way, considering that at high energy the longitudinal c.m. variable X_F is approximately equal to the laboratory energy fraction X_{lab} in the forward region, up to terms of the order of $(m_\perp/E_0)^2$:

$$\begin{aligned} r &\sim \frac{P_\perp}{X_F^{\pi,K} E_0} H_{prod} \\ &\propto \frac{P_\perp}{X_F^{\pi,K} E_0} \left(\log \sigma_{n-Air}^{inel} + const. \right) \end{aligned} \quad (2)$$

where a simple exponential atmosphere profile has been used in the last expression.

Of course, in the case of underground experiments, muon propagation in the rock is also a fundamental aspect of calculation, but it is a factorizable ingredient, not to be discussed in this work. A discussion of this topic can be found in [18]. It can just be mentioned that, even for large depths, although the scattering in the rock is quantitatively important, the simulation results show that the amount of this deviations it is not yet enough to obscure the influence of P_\perp in the lateral distribution of the surviving muon component.

The energy filter provided by the rock, imposes a threshold on the muon energy, and therefore also on its parents’ energy. This introduces some selection effects. Considering for example the case of Gran Sasso laboratory. There, the minimum rock overburden is about 3100 hg/cm² (in the direction of Campo Imperatore, where EAS-TOP is located). That depth corresponds to an energy threshold for muons of about $E_\mu^{thr} \sim 1.3$ TeV. The average energy of parent pions must be

$$\langle E_\pi \rangle \simeq \frac{E_\mu^{thr}}{0.5(1 + \frac{m_\mu^2}{m_\pi^2})} \simeq 1.6 \text{ TeV} \quad (3)$$

When considering the first primary interaction of a nucleon, at energy E_0 , a threshold in muon energy is thus equivalent to a threshold in $X_F \simeq X_{lab} = \frac{E_\pi}{E_0}$, which for “low” E_0 values (a few TeV) can be close to 1, *i.e.* in the very forward region. In that cases, in practice only muons from the first generation in the cascade are detected, and the primary interaction is really investigated. At fixed threshold, for increasing primary energy, the average X_{lab} of parents at first decreases, and then exhibits a smooth rise, when more and more cascade generation can provide mesons above threshold. This is shown in Fig.1 for parent pions from proton and Fe primaries, in the case of 3400 hg/cm², at 30° of zenith angle.

Since below 10 TeV, the composition of primaries contributing to TeV muons is strongly dominated by protons, this selection effect is being exploited in the coincidence experiment of EAS-TOP and MACRO to investigate the differences between interaction models in the fragmentation region[19].

In this limited discussion the interesting question of prompt muons from the decay of heavy flavored mesons will be neglected. However, it is recognized that this production is indeed a very small fraction of TeV muons surviving underground (see for instance ref. [26]), and there is debate on the real possibility of a positive detection of this component.

3 Monte Carlo generators

After the first fundamental work of Elbert[20], an important paper concerning the simulation of muons detected deep underground is that of ref. [21], where parameterizations as a function of energy per nucleon, zenith angle and rock depth were presented, following the method already pointed out in[20]. The calculations were performed using, as interaction model, the “splitting Hillas’ algorithm”[22]. This algorithm is indeed simple, perfectly preserving Feynman scaling and does not provide any information about the transverse structure of the showers. More realistic predictions were obtained with the development of the HEMAS code[23], which was explicitly designed to provide a dedicated tool for the high energy muon component (above 500 GeV), in view of the experimental activity at Gran Sasso laboratory. The hadronic interaction model of HEMAS is based on the parameterizations of collider data, mostly UA5[25], following a picture in which clusters of particles were formed in the nucleon–nucleon collisions, eventually decaying into ordinary mesons. Effects due to the nuclear nature of the target, as measured in heavy ion physics, are used to correct multiplicity, transverse momentum, etc.

The most noticeable differences coming from these collider parameterizations concern two aspects:

1. the larger fluctuations of muon multiplicity, in connection to the negative binomial multiplicity distribution of produced mesons
2. the transverse distribution of muons, following the power law distribution related to that of P_\perp and its correlation with energy and multiplicity.

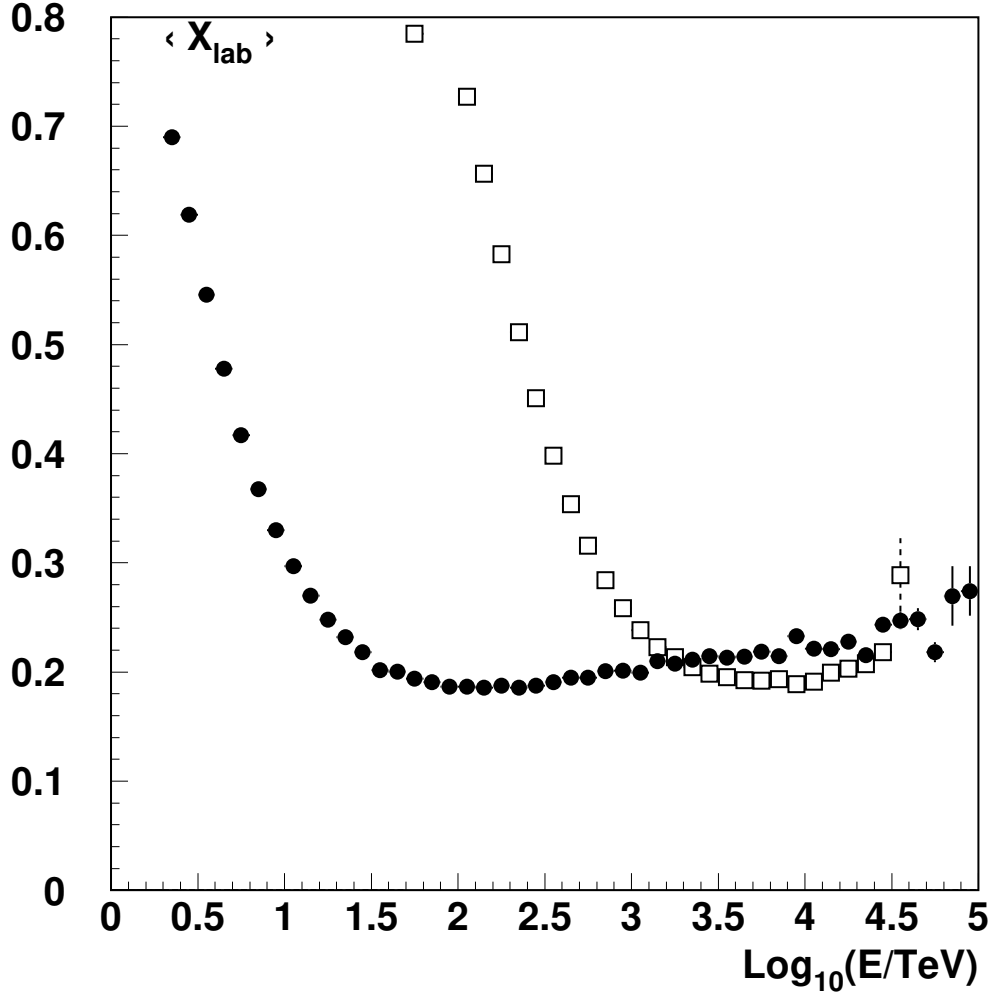


Figure 1: Monte Carlo calculation of Average X_{lab} of parent pions of muons detected after 3400 hg/cm^2 of standard rock, at 30° of zenith angle, for proton (black circles) and iron nuclei (open squares) primaries.

The first analyses by MACRO[9, 24] could establish the much better description of data provided by HEMAS with respect to the previous parameterizations of [21]. It must be quoted that also the recent analysis of KGF made use of similar collider parameterizations.

In any case, this type of codes have still a weak point. The application to cosmic rays necessarily requires some extrapolation, in particular towards the high X_F values, and this procedure has always some degree of arbitrariness. Also, in the construction of parameterizations, important correlations among variables might be lost. These are some of the reason that have driven people to look for “theoretically inspired” models, with a limited number of parameters and a phenomenological framework as a guidance. A rather remarkable success in hadronic physics seems to be achieved by the Dual Parton Model[27] (DPM). This approach makes use of concepts derived from the mathematical requirements of scattering theory, as unitarity and analyticity together with color flow and parton idea and topological expansion of QCD. Such concepts can be formulated in the framework of relativist quantum field theory, according to the Regge–Gribov approach[28]. The extension from nucleon–nucleon to nucleon–nucleus and nucleus–nucleus is achieved according to the Glauber multiple scattering formalism[29]. A last fundamental ingredient of all these models is the “hadronization” algorithm, where parton strings produced in the scattering process are converted into ordinary particles. Some authors make use of the hadronization Lund models[30].

In practice, many different variations exist of these basic ideas, and also many different practical implementation have been developed in different numerical codes. Some of these have been successfully interfaced to the general purpose shower code CORSIKA, as already mentioned in the introduction. A detailed description of these models can be found only in the original literature, however the most important features are the following¹.

1. HDPM[3]. This is the original interaction package contained in CORSIKA, where parameterizations of the main results of DPM are contained. It will not be considered in the following.
2. SIBYLL[32]. It was explicitly developed for cosmic ray application. It contains DPM ideas, but the present version is deeply based on the minijet production as calculable from QCD, providing all the rising part as a function of energy of the nucleon–nucleon cross section. The soft part is constant. A Lund code for hadronization is used.
3. DPMJET[32]. It is based on the “Two component” DPM, i.e. both soft processes and hard QCD scattering are unitarized together. The soft part assumes the “super-critical pomeron” so that the soft contribution of the cross section is not constant but rises as $s^{0.08}$. Multi-Pomeron exchange is possible. A specific point of merit of this code is the inclusion of dedicated algorithms to treat nuclear effects. Also DPMJET makes use of a Lund hadronization code. It must be mentioned that this interaction model has been also chosen for a new version of HEMAS[35], called

¹CORSIKA makes use of the GHEISHA[31] parameterized model below 80 GeV incident hadron energy. This is irrelevant for TeV muons.

HEMAS–DPM, again specifically devoted to high energy muons. This is presently in use by the MACRO experiment, and preliminary results are presented at this conference[34]. From the point of view of results, no significant differences with respect to those achieved inside CORSIKA are expected, although the comparison of results from the same interaction model from two different shower codes would be a technically interesting issue. This will be discussed in [16].

4. QGSJET[36]. It is based on the “Quark Gluon String” model[37]. It is very similar to DPMJET as far the pomeron parameters are concerned. It also includes the contribution of perturbative QCD. At present there are important differences with respect to DPMJET in the way in which soft and hard scattering are merged together.
5. VENUS[38]. Originally developed for accelerator physics. It contains DPM with the supercritical pomeron, and the addition of some specific features concerning color exchange processes. It introduces secondary interaction of strings before hadronization. The version at present in CORSIKA does not yet include the contribution of minijets.

In the following results concerning high energy muons from some of these choices will be compared. For some specific issues the with the original HEMAS code will be also shown.

4 Particle Production in p–Air single interaction

The first approach in the comparison of models for shower calculation is the analysis of the features of primary interaction. In principle, one has to study the primary interaction in both nucleon–Air and nucleus–Air collisions. However, for simplicity, the nucleon–Air interaction can be considered as the basic representative ingredient of the models. The extension to nucleus–nucleus interaction according to the Glauber model could be, in principle, a common part to all codes. However, a check of how this is realized in practice is mandatory and will be addressed in future. For the comprehension of shower development, the study of meson–Air interaction would be also important. An exhaustive examination would require a ponderous dissertation, that goes beyond the present possibility. The discussion will be limited to the inelastic cross section, the X_{lab} and the P_{\perp} distributions.

4.1 The inelastic cross section

In Fig. 2, the p–Air inelastic cross section as a function of laboratory energy is shown for some of the considered models, in the relevant energy range accessed with muons detected deep underground.

There are significative differences in the knee region (VENUS seems to depart more from the other ones), but also at \sqrt{s} values where good p–p data are available. Here the SIBYLL cross section seems to exhibit the major deviation. Presumably, this can be

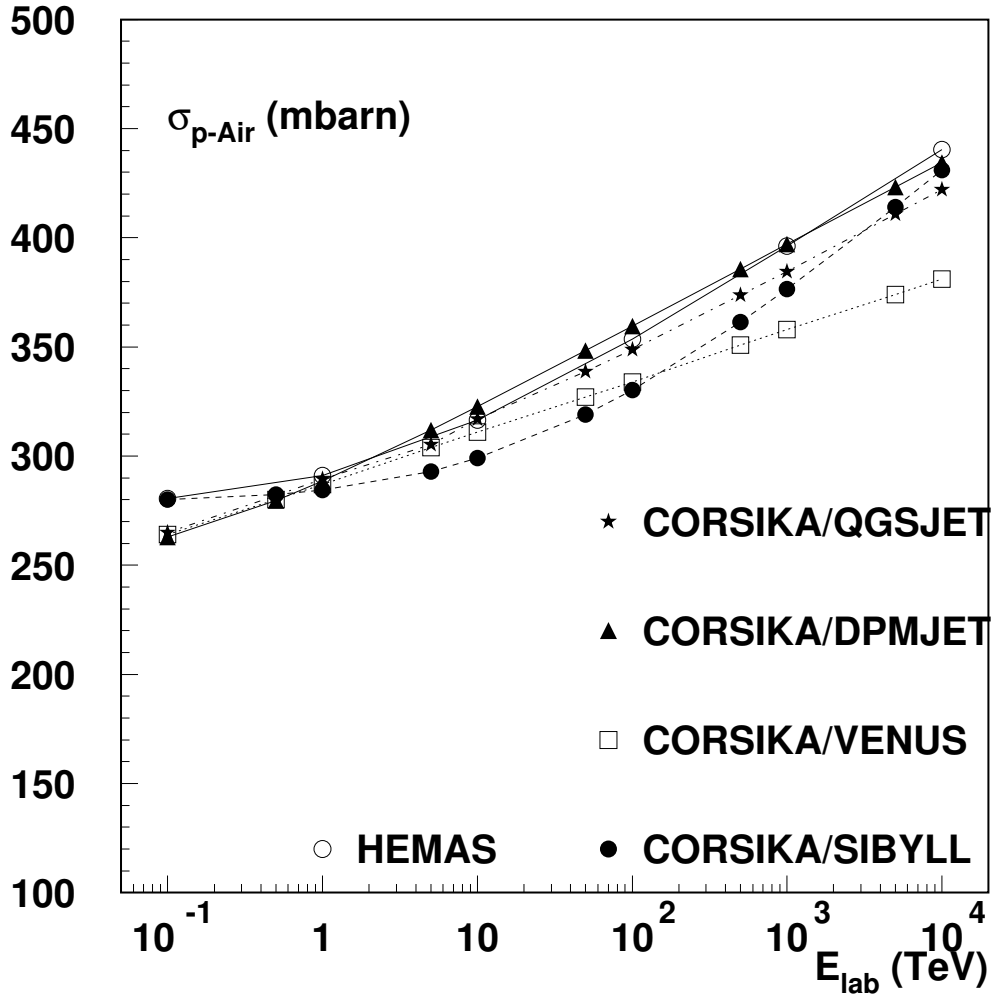


Figure 2: Inelastic p–Air cross section as a function of laboratory energy for some of the considered Monte Carlo models.

attributed to a non correct inclusion of diffractive events in the Glauber calculation[39], and in the next version of SIBYLL this problem will be corrected. These differences in cross section will be reflected by different average interaction heights and some change in the muon production height.

4.2 Inclusive distributions and the Spectrum-weighted moments

As a significant example of possible difference between codes, Fig. 3 shows the X_{lab} distribution of charged pions produced in p–Air collisions at 200 TeV in the laboratory frame, for 3 different codes: DPMJET (continuous line), QGSJET (dashed) and VENUS (dotted). The difference of DPMJET with respect the other codes at large X is due to a particular mechanism of Lund fragmentation (JETSET 7.3) of the fast valence “diquark”² in the projectile, in the case of positive pions (“popcorn” effect[40]). No effect of this kind is instead possible for kaon production, where strange quark are not presented in the valence quarks, or diquarks, of the incoming nucleon. This mechanism is not included in the other MC codes. This feature has indeed relevance in the yield of high energy muon. It is important to notice that, apart from the region near $X_{lab}=0$ and $X_{lab}=1$, these Regge–Gribov model exhibit a substantial Feynman scaling. Therefore these features are preserved in a wide range of energies.

In the current literature, some emphasis has been given to the “spectrum-weighted” moments, defined, for instance in case of pion production, as

$$Z^\pi = \int_0^1 (X_{lab})^{\gamma-1} \frac{dN^{p+Air \rightarrow \pi+X}}{dX_{lab}} dX_{lab} \quad (4)$$

where γ is spectral index of primary nucleons. Such a function give a measurement of the inclusive particle yield in cosmic ray showers after the integration over the energy spectrum[41]. In principle, the high energy muon yield is proportional to those values. However, the comparison of Z-moment from different codes, as that shown in Fig. 4, cannot give completely meaningful information when the inelastic cross sections are different. In fact, a larger Z factor (as in the case of SIBYLL) will not give a larger muon yield if the production height is lower, so that available length for decay is smaller.

It is also interesting to inspect the behaviour of the energy fraction K_B carried away by the leading baryon in p–Air collisions as a function of primary energy. This is shown in Fig.5. It can be seen how the HEMAS code exhibits a different behaviour from other representative models of the QGS and DPM kind, where elasticity smoothly decreases with energy. In this respect, it is worthwhile to remark what stated in ref.[42] about the cluster models. Such approaches have the general tendency to produce events which become increasingly elastic as energy increase³. In the same reference it was shown how QGSJET and DPM model represent interactions on nuclear targets in a way which is

²*i.e.* the projectile after the stripping of one valence quark

³It has been suggested that a less unbiased way to look at elasticity would be to consider $K_{B-\bar{B}}$, where anti-baryons are taken with the minus sign.

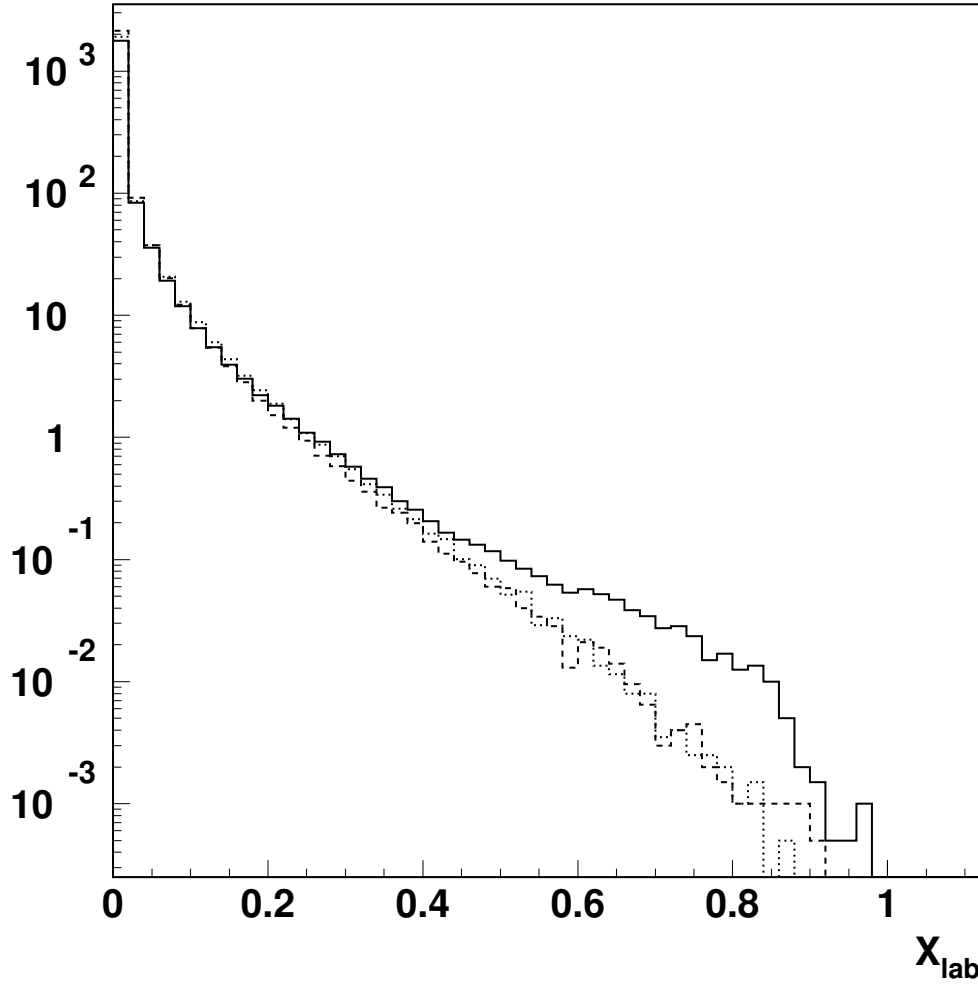


Figure 3: X_{lab} distribution for charged pions produced in p–Air collisions at 200 TeV in the laboratory frame for DPMJET (continuous line), QGSJET (dashed) and VENUS (dotted).

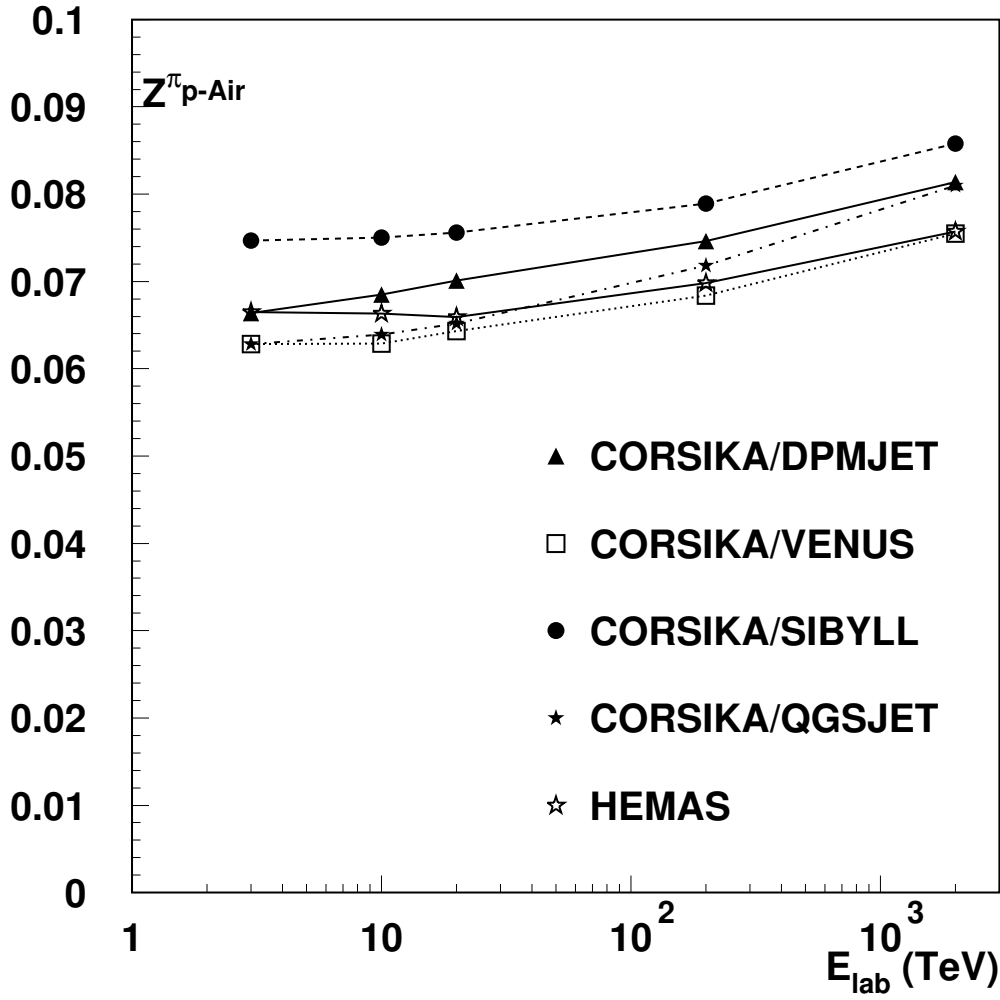


Figure 4: Comparison of Z moments for charged pion production as a function of energy, for different codes.

consistent with low energy data. It can be important to notice how a model like the quoted Hillas' algorithm, in its original form, would give a constant $K_B=0.5$.

A few remarks are necessary as far as the P_\perp distribution is concerned. The phenomenological framework of the Regge–Gribov theories, by its nature, provides only predictions for the longitudinal properties of the interaction. The transverse structure leading to the specific P_\perp distribution is not constrained by the theory, but for the higher P_\perp phenomena, where perturbative QCD can be used (of small relevance in the primary energy region addressed in general by the underground experiment). Once again, the model builders have to be guided mostly by experimental data, introducing *a-priori* determined functional forms with their additional parameters. Again, as a typical example, the P_\perp distribution of charged pions produced in p–Air collisions at 200 TeV laboratory energy, as obtained in different models is shown in Fig.6.

It can be pointed out how all the considered models produce P_\perp distributions which, following the experimental results at colliders, can be fitted with a power law spectrum. It can be also noticed how HEMAS and DPMJET give very close results, predicting larger tails than the other models at relatively high values of P_\perp .

5 Shower Calculations

Test simulation runs of EAS development have been performed, choosing typical parameters for the experimental situation at Gran Sasso laboratory. According to the logic followed so far, results are presented here only for the case of proton primaries. Runs have been performed at different fixed energies, for fixed angles (30° zenith and 190° azimuth), setting the observation level for EAS at 2000 m a.s.l., and with the geomagnetic field specific for the site. The chosen direction corresponds to the typical one from which the underground halls see the EAS–TOP array. Propagation of TeV muons in rock has been calculated by means of the PROPMU code[43] for the corresponding thickness of 3400 hg/cm² of standard rock. In Table 1 the average yield of muons as measured at the surface ($E_\mu \geq 1$ TeV) is reported, together with that of the survived muons underground.

A comparison of muon yields in showers from protons and primary nuclei is shown, for example at 2000 TeV total energy, in Table 2. The shape of the muon multiplicity distributions from the different models are very similar, as, for instance, in the example of Fig. 7, from p–Air collision at 2000 TeV.

As far as the underground muon yield is concerned, it can be seen how these predictions are in general close one to the other. The most relevant percentage differences, for a given threshold on muon energy, are noticeable near the corresponding threshold energy for primaries. In this context, it can be important to remind the considerations expressed in Sect. 2, about the importance of high X_F region in meson production, where the distribution from different models depart more one from another.

A summary concerning the quantities affecting the transverse structure of the high energy muon component is reported in Table 3. These are the average depth of the first

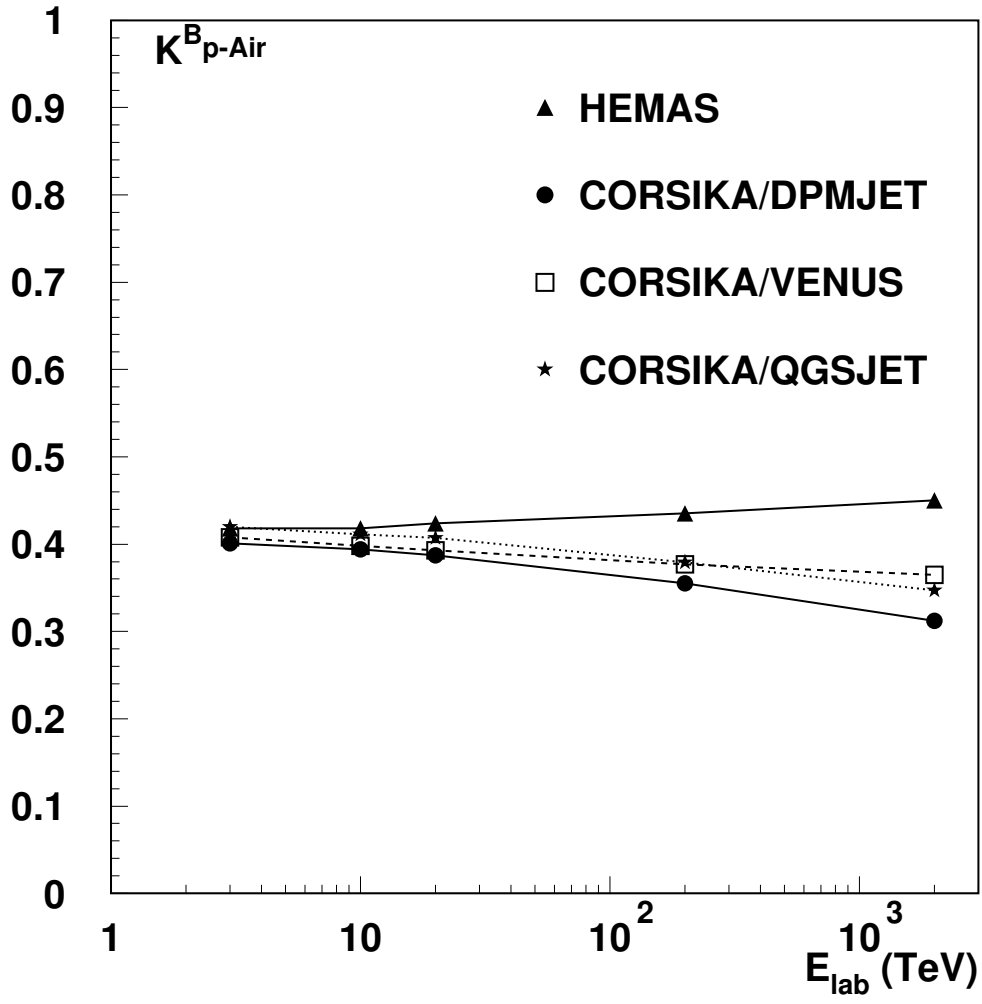


Figure 5: Comparison of the energy fraction carried away by leading nucleons in p–Air collisions as a function of laboratory energy, for different models.

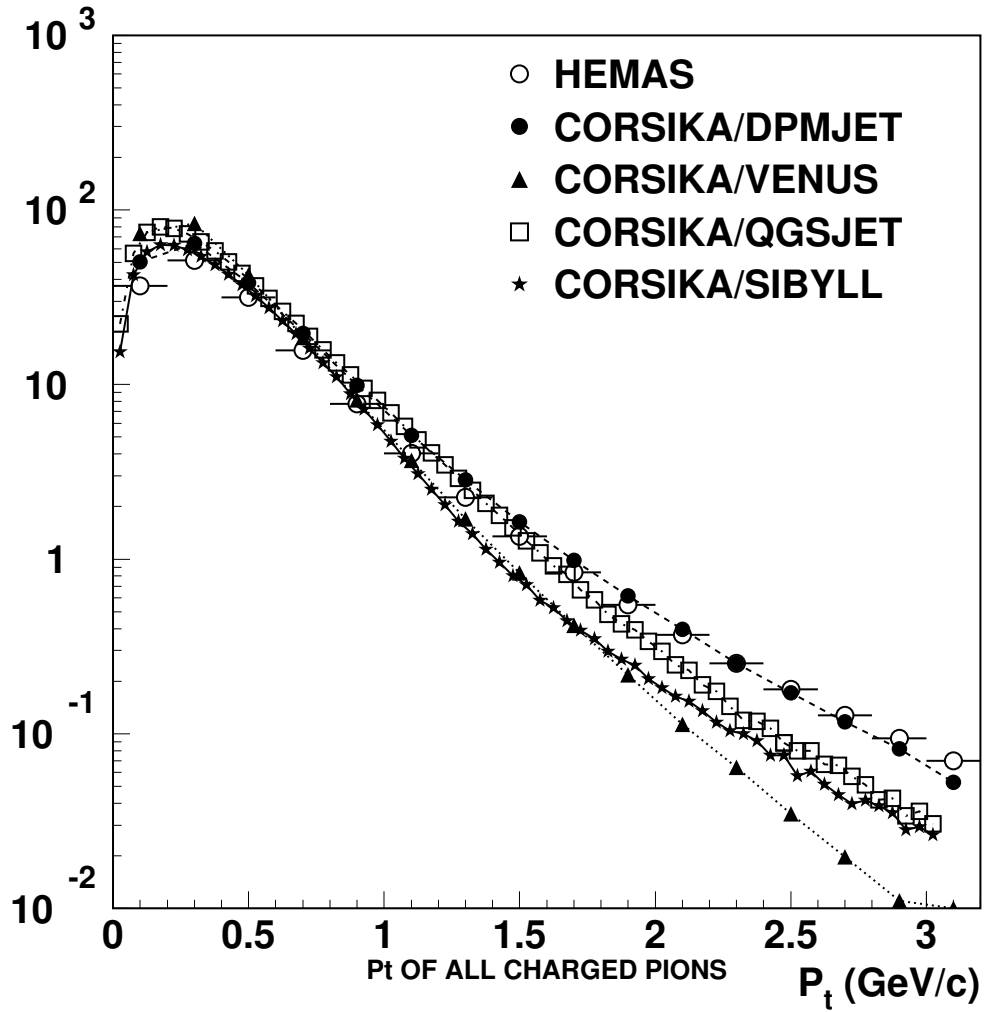


Figure 6: Comparison of P_{\perp} distributions of charged pions produced in p–Air collisions at 200 TeV laboratory energy, for different models.

Table 1: Comparison of average TeV muon yield at 2000 m a.s.l. and of the no. of muons surviving underground, after 3400 hg/cm², produced in proton induced showers at different energies. The same muon transport code has been applied in all runs. The relative statistical error on the reported figures is of the order of 5

p-Air, 3 TeV		
Code	$\langle N_\mu(E \geq 1 \text{ TeV}) \rangle$	$\langle N_\mu \rangle$ survived undergr.
HEMAS	0.0027	0.00049
CORSIKA/DPMJET	0.0035	0.00059
CORSIKA/QGSJET	0.0018	0.00015
CORSIKA/VENUS	0.0028	0.00031
CORSIKA/SIBYLL	0.0042	0.00056
p-Air, 10 TeV		
Code	$\langle N_\mu(E \geq 1 \text{ TeV}) \rangle$	$\langle N_\mu \rangle$ survived undergr.
HEMAS	0.064	0.015
CORSIKA/DPMJET	0.055	0.016
CORSIKA/QGSJET	0.056	0.015
CORSIKA/VENUS	0.057	0.015
CORSIKA/SIBYLL	0.064	0.018
p-Air, 20 TeV		
Code	$\langle N_\mu(E \geq 1 \text{ TeV}) \rangle$	$\langle N_\mu \rangle$ survived undergr.
HEMAS	0.182	0.048
CORSIKA/DPMJET	0.142	0.049
CORSIKA/QGSJET	0.153	0.052
CORSIKA/VENUS	0.150	0.049
CORSIKA/SIBYLL	0.153	0.053
p-Air, 200 TeV		
Code	$\langle N_\mu(E \geq 1 \text{ TeV}) \rangle$	$\langle N_\mu \rangle$ survived undergr.
HEMAS	1.29	0.47
CORSIKA/DPMJET	1.17	0.49
CORSIKA/QGSJET	1.17	0.48
CORSIKA/VENUS	1.28	0.52
CORSIKA/SIBYLL	1.11	0.44

Table 2: Comparison of average TeV muon yield at 2000 m a.s.l. and of the no. of muons surviving underground, after 3400 hg/cm², produced in showers induced by different primary nuclei at 2000 TeV total energy.

p–Air, 2000 TeV		
Code	$\langle N_\mu(E \geq 1 \text{ TeV}) \rangle$	$\langle N_\mu \rangle$ survived undergr.
HEMAS	6.44	2.55
CORSIKA/DPMJET	6.90	2.84
CORSIKA/QGSJET	6.79	2.80
CORSIKA/VENUS	7.43	3.09
CORSIKA/SIBYLL	5.99	2.48
He–Air, 2000 TeV		
Code	$\langle N_\mu(E \geq 1 \text{ TeV}) \rangle$	$\langle N_\mu \rangle$ survived undergr.
HEMAS	9.51	3.75
CORSIKA/DPMJET	9.61	3.94
CORSIKA/QGSJET	8.89	3.66
CORSIKA/VENUS	10.26	4.23
CORSIKA/SIBYLL	8.67	3.59
Fe–Air, 2000 TeV		
Code	$\langle N_\mu(E \geq 1 \text{ TeV}) \rangle$	$\langle N_\mu \rangle$ survived undergr.
HEMAS	16.42	5.61
CORSIKA/DPMJET	15.72	5.86
CORSIKA/QGSJET	15.87	5.74
CORSIKA/VENUS	16.92	6.17
CORSIKA/SIBYLL	15.15	5.57

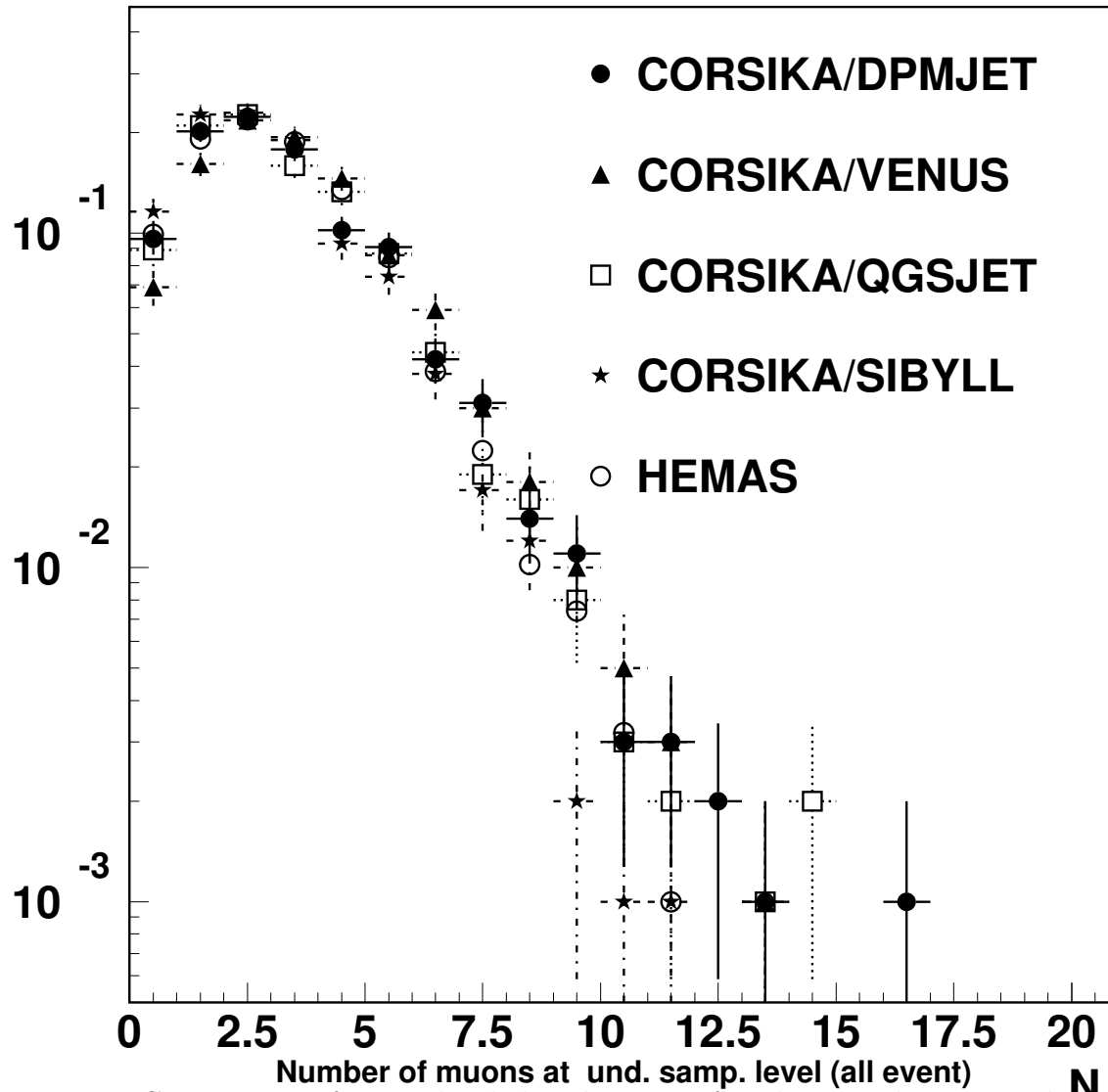


Figure 7: Comparison of normalized distributions of underground muon multiplicity from p–Air collisions at 2000 TeV laboratory energy, 30° zenith angle, and 3400 hg/cm² depth, for different models.

interaction X_{first} , $\langle P_{\perp} \rangle$ for pions coming from the first interaction, the average slant production height H_{μ} of muons survived underground (the decay height of their parent mesons⁴), the average distance of muons from shower axis underground ($\langle R \rangle$) and the average muon pair separation for multiple muon events ($\langle D \rangle$).

In the energy range around hundreds of TeV, to which most of data taken at Gran Sasso laboratory belong, the resulting differences in the average muon separation do not exceed 20%. These discrepancies seem to reduce at higher energy, while they appear much larger a few tens of TeV. DPMJET is probably the only model predicting a higher average separation than HEMAS. A precise analysis of the reasons leading to those differences in the models is complicated, however, it is important to notice that, in fact, HEMAS gives in general higher values of average P_{\perp} with respect to the other models. The only exception is indeed DPMJET, which, as mentioned before, has a particular attention to the reproduction of nuclear effects affecting the transverse momentum, as measured in heavy ion experiments. On the other hand, the effect on this larger P_{\perp} on the lateral distribution of muons is moderated in HEMAS by a deeper penetration of showers, giving in general a somewhat smaller average height of meson production. Similar features in the comparison of models are also obtained for nuclear projectiles. The data analysed by MACRO[24, 10] favour the HEMAS simulation, however a comparison of the same data with other models is still missing.

6 Conclusions

It has been shown that, as far as TeV muons are concerned, differences in the predicted yield are not enormous, although they exist. So far, the published analyses from different experiments have been mostly based on a given specific model. In the light of the present results, it is instead recommended that each group should consider more than one model for the interpretation in terms of spectrum and composition of primaries. In particular, it would be highly desirable that the set of considered simulation codes for event generation would be the same for every collaboration. This of course requires a considerable effort to the experimental groups, however it appears necessary in view of a sensible comparison of the different results, which at present are sometimes still controversial, despite the high quality reached in the detector and analysis techniques. This is valid not only for the underground experiments, but also for EAS array. In this respect, more complete results on code comparison will be provided in a next work[16]. The results presented at this conference by the MACRO experiment[34], are an important example in the in the case of DPMJET, which provides a larger muon yield underground. suggested direction: the analysis of primary spectrum, originally based on HEMAS, can converge to significantly different values in the case of DPMJET, which provides a larger muon yield underground.

A fundamental question is if it is possible an experimental discrimination of hadronic interaction models on the basis of cosmic ray data themselves. As far as high energy muons

⁴CORSIKA does not allow to access directly to the production height of parent mesons, which would be more interesting for our purposes

Table 3: Comparison of a few relevant quantities concerning the lateral distribution of underground muons at the depth of 3400 hg/cm², from proton primaries at 20, 200 and 2000 TeV, 30° zenith angle.

p–Air, 20 TeV					
Code	$\langle X_{first} \rangle$ (g/cm ²)	$\langle P_{\perp} \rangle \pi^{\pm}$ (GeV/c)	$\langle H_{\mu} \rangle$ (km)	$\langle R \rangle$ (m)	$\langle D \rangle$ (m)
HEMAS	51.4	0.40	24.1	7.9	12.7
CORSIKA/DPMJET	44.4	0.42	25.6	10.1	13.9
CORSIKA/QGSJET	45.7	0.39	24.3	7.3	10.0
CORSIKA/VENUS	48.3	0.35	24.5	7.4	8.3
CORSIKA/SIBYLL	50.9	0.37	23.5	7.2	11.5
p–Air, 200 TeV					
Code	$\langle X_{first} \rangle$ (g/cm ²)	$\langle P_{\perp} \rangle \pi^{\pm}$ (GeV/c)	$\langle H_{\mu} \rangle$ (km)	$\langle R \rangle$ (m)	$\langle D \rangle$ (m)
HEMAS	56.1	0.44	20.6	5.3	8.0
CORSIKA/DPMJET	53.9	0.43	21.7	6.2	8.8
CORSIKA/QGSJET	52.8	0.41	21.4	5.5	7.8
CORSIKA/VENUS	60.2	0.36	20.9	5.3	7.5
CORSIKA/SIBYLL	55.2	0.41	20.2	5.2	7.3
p–Air, 2000 TeV					
Code	$\langle X_{first} \rangle$ (g/cm ²)	$\langle P_{\perp} \rangle \pi^{\pm}$ (GeV/c)	$\langle H_{\mu} \rangle$ (km)	$\langle R \rangle$ (m)	$\langle D \rangle$ (m)
HEMAS	63.0	0.50	16.3	4.1	6.0
CORSIKA/DPMJET	60.0	0.42	18.5	4.9	6.4
CORSIKA/QGSJET	63.1	0.44	17.7	4.2	5.6
CORSIKA/VENUS	66.7	0.36	16.8	4.1	5.3
CORSIKA/SIBYLL	60.3	0.44	17.0	4.4	5.6

are concerned, the answer is not yet certain. However, there are promising interesting measurements which cover the range of primary energy below few tens of TeV. The coincidence experiment Ne- N_μ at Gran Sasso[19] has been already mentioned. The same collaborations are now preparing the analysis of coincidences between Cherenkov signal and TeV muons underground[44]. This would allow the study of TeV muon yield as a function of energy in the threshold region. It is important to remark that, although these check can be done in a limited and relatively low energy, they are in any case important to understand features, like the shape of X_{lab} distribution which, as discussed before, are essentially preserved in a wide energy range.

Last but not least, the quality of the different models can be debated just on phenomenological bases. Despite the common basic language, the presently available “theoretically inspired” models do still contain many free parameters and rather different choices for the algorithmic solutions. Hopefully, if future data on soft physics from LHC will be available (after year 2005), these might be helpful in reducing some of the uncertainties in the interaction features and in the shower calculations, as far as the energy region of the knee, and above, is concerned.

Acknowledgments

The author is indebted to M. Ambrosio, C. Aramo, M. Carboni, C. Forti and J. Ranft for the technical help with the codes and for the critical discussions.

References

- [1] A.A. Watson. Nucl. Phys. B (Proc. Suppl.) **60B** (1998) 171
- [2] P. Doll et al., KFK 4686, Karlsruhe report, 1990
- [3] J.N. Capdevielle et al., Karlsruhe report KFK 4998 (1992).
- [4] J. Knapp, D. Heck and G. Schatz, Karlsruhe report FZKA 5828 (1996).
- [5] J. Knapp, these proceedings.
- [6] H.E. Bergeson et al., Phys. Rev. Lett. **35** (1975) 1681.
- [7] G. Bologna et al., Il Nuovo Cimento **8C** (1985) 76.
- [8] Ch. Berger et al., Phys. Rev. **D40** (1989) 2163.
- [9] MACRO Collaboration, Phys. Rev. D **46** (1992) 895.
- [10] MACRO Collaboration, M. Ambrosio et al., Phys. Rev. **D56** (1997) 1407 and 1418.
- [11] SOUDAN2 Collaboration, Phys. Rev. **D55** (1997) 5282.

- [12] H.R. Adakar et al., Phys. Rev. **D57** (1998) 2653.
- [13] LVD Collaboration, Il Nuovo Cimento **105A** (1992) 1815 and Astropart. Phys. **2** (1994) 103.
- [14] EAS-TOP Collaboration, Nucl. Instr. & Meth. **A277** (1989) 23.
- [15] EAS-TOP and MACRO Collaborations, Phys. Lett., **B337** (1994) 376.
- [16] C. Aramo, M. Ambrosio, G. Battistoni and C. Forti, work in preparation.
- [17] T.K. Gaisser, Proc. Vulcano Workshop 1992 on “Frontier Objects in Astrophys. and Particle Phys.”, **40**, (1993) 433.
- [18] G. Battistoni et al., Nucl. Instr. & Meth. **A394** (1997) 136.
- [19] EAS-TOP and MACRO Collaborations, Proc. 25th I.C.R.C., Durban, **6** (1997) 85.
- [20] J.W. Elbert, Proc. DUMAND Summer Workshop, Vol. **2** (1978) 101; J.W. Elbert et al., Phys. Rev. **D27** (1983) 1448.
- [21] T.K Gaisser and T. Stanev, Nucl. Instr. & Meth. **A235** (1985) 183.
- [22] A.M. Hillas, Proc. 17th I.C.R.C., Paris, **8** (1981) 193.
- [23] C. Forti et al., Phys. Rev. **D42** (1990) 3668.
- [24] MACRO Collaboration, S.P. Ahlen et al., Phys. Rev. **D46** (1992) 4836.
- [25] G.J. Alner et al., Physics Letters **167B** (1986) 476.
- [26] G. Battistoni et al., Astropart. Phys. **4** (1996) 351.
- [27] A. Capella et al., Phys. Rep. **236** (1994) 225.
- [28] V.N. Gribov, Sov. Phys. JETP **26** (1968) 414; V.N. Gribov and A.A. Migdal, Sov. J. Nucl. Phys. **8** (1969) 583.
- [29] R.J Glauber and G. Matthiae, Nucl. Phys. **B21** 135.
- [30] H. Bengtsson and T. Sjöstrand, Comput. Phys. Commun. **46** (1987) 43.
- [31] H. Fesefeldt, Aachen preprint PITHA 85/02 (1985).
- [32] R.S. Fletcher et al., Phys. Rev. **D50** (1994) 5710.
- [33] J. Ranft, Phys. Rev. **D51** (1995) 64.
- [34] O. Palamara for the MACRO collaboration, these proceedings.
- [35] G. Battistoni et al., Astropart. Phys. **3** (1995) 157.

- [36] N.N. Kalmikov et al, Physics of Atomic Nuclei **58** (1995) 1728.
- [37] A.B. Kaidalov et al., Yad. Fiz. 43 (1986) 1282.
- [38] K. Werner, Phys. Rep. **232** (1993) 87.
- [39] T. Stanev, these proceedings.
- [40] T. Sjöstrand, CERN-TH.6488/92 (1992)
- [41] R.S. Fletcher et al., Proc. 23rd I.C.R.C., Calgary, **4** (1993) 40.
- [42] G.M. Frichter, T.K. Gaisser and T. Stanev, astro-ph/9704061 and Phys.Rev. **D56** (1997) 3135.
- [43] P. Lipari and T. Stanev, Phys. Rev. **D44** (1991) 3543.
- [44] C. Morello for the EAS-TOP collaboration, these proceedings.